System-level Analysis of Chilled Water Systems Aboard Naval Ships

Hessam Babaee, Julie Chalfant,
Chryssostomos Chryssostomidis
MIT Sea Grant
Massachusetts Institute of Technology
Cambridge, MA
Email: babaee@mit.edu

Amiel B. Sanfiorenzo †
Puget Sound Naval Shipyard
and Intermediate Maintenance Facility
Bremerton, WA

***Abstract*—A thermal management simulation tool is required to rapidly and accurately evaluate and mitigate the adverse effects of increased heat loads in the initial stages of design in all-electric ships. By reducing the dimension of Navier-Stokes and energy equations, we have developed one-dimensional partial differential equation models that simulate time-dependent hydrodynamics and heat transport in a piping network system. Besides the steady-state response, the computational model enables us to predict the transient behavior of the cooling system when the operating conditions are time-variant. As a demonstration case, we have performed a thermal analysis on a realistic naval ship.**

I. Introduction

Advances in sensors and weapons for modern naval combatants are resulting in orders of magnitude increases in power draw, which place unprecedented demands on cooling systems; this trend is expected to continue for the foreseeable future. As a result, the design of the cooling system can no longer be left to the later stages of design, but must be considered much earlier. A simulation tool is required to assess the impact of the cooling system design on the overall ship in the early stages.

In this paper, we present a system-level simulation tool that provides rapid design, modeling and analysis of chilled water cooling systems using first principles. We begin with a short list of required inputs appropriate to the early stages of design:

1) Basic ship geometry including ship length and beam.
2) The locations of major bulkheads and decks.
3) The locations, load value, and vital/non-vital designation of heat loads.

The software contains specifications of many existing cooling system components such as chillers and heat exchangers, including equipment in current use and new *state-of-the-art* components. The modular nature of the software also provides the capability to insert additional components, thus enabling the analysis of the impact of newly developed technologies.

Using the input described above and the user's selection of components and topology templates, the program automatically provides a system design which includes the following specifications:

1) Thermal zone extents.
2) Piping path and diameter.
3) Specifications and locations of chillers, heat exchangers, pumps and valves.

The framework of the system modeling is based on the work of Sanfiorenzo [1] and Fiedel [2].

Following system design, the simulation tool performs comprehensive static and transient hydrodynamic and thermal analyses, and computes temperature, pressure and velocity across the cooling network. Our formulation is fast to evaluate and is suitable for exploring various configurations in the initial stages of design. As a demonstration case, we have performed static and transient analysis for a naval ship with realistic specifications.

II. Quasi one-dimensional transient model

A. Modeling assumptions

One-dimensional models of flow in elastic pipes are derived by reducing the dimensionality of the full Navier-Stokes equations under the following assumptions:

1) Quasi one-dimensional flow: this assumption assumes that the tangential and radial velocity components are zero, *i.e.* $u_r(r,\theta,x,t) = u_\theta(r,\theta,x,t) = 0$, adopting a cylindrical coordinate system. As a result of this assumption, using the full Navier-Stokes equations, one can show that
$$\frac{\partial p}{\partial r} = \frac{\partial p}{\partial \theta} = 0.$$
2) Axial symmetry: this assumes that any quantity such as $u(r,\theta,x,t)$ is independent of the angular

This work is supported by the Office of Naval Research N00014-14-1-0166, ESRDC – Designing and Powering the Future Fleet, and MIT Sea Grant College Program under NOAA Grant Numbers NA14OAR4170077 and NA10OAR4170086.

†LT Sanfiorenzo was a graduate student with the MIT Design Laboratory when this work was accomplished.

978-1-4799-1857-7/15/$31.00 ©2015 IEEE

location θ, and therefore $u := u(r,x,t)$. This assumption becomes more accurate if the local curvature of the pipe is small. For instance, in cases where flow undergoes a sharp turn, such as a 90° bend or a junction, the axial symmetry may not be a valid assumption. In those cases, we model the component (*i.e.* bend, junction, etc.) separately.

3) Fixed radial dependence: the axial velocity profile is assumed to be in the form of

$$u_x(r,x,t) = u(x,t)g(r)$$

where $u(x,t)$ is the mean of the profile and thus $\int_0^{r_i} \pi g(r) r dr = \pi r_i^2$, where r_i is the internal radius of the pipe. The choices for radial dependence functions depend on the flow condition. For instance, the Poiseuille flow profile may be assumed for a laminar flow condition, or an experimental profile may be considered for a turbulent flow condition. As will be demonstrated later in the paper, the explicit profile of $g(r)$ does not appear in the mathematical modeling. However $g(r)$ directly affects the friction factor as different choices of $g(r)$ determine the shear stress at the pipe wall.

4) Incompressible flow: we assume that the working fluid is incompressible. Therefore, the internal energy e is expressed as:

$$e = c_p T,$$

where c_p is the specific heat capacity.

5) Negligible kinetic energy: the kinetic energy is neglected as it has significantly smaller values than the internal energy of liquids such as water. Thus $e + u^2/2 \simeq e$.

6) Negligible conduction: in most realistic cases, axial and radial conduction terms are negligible compared to the advection terms.

The first three assumptions mentioned above are analogously used for temperature, and thus temperature can be expressed as $T := T(x,t)h(r)$, where $T(x,t)$ is the mean temperature.

B. Mathematical Modeling

1) Hydrodynamics: To model the propagation of transient flow in pipes, both the compressibility of the liquid and the elasticity of the pipe must be modeled. Local increase in fluid pressure results in local enlargement of the pipe cross section area. In general the unknown variables are pressure $p(x,t)$, axial velocity $u(x,t)$ and the cross sectional area $A(x,t)$. A purely elastic model provides a pressure-area relation. The Laplace's law provides such a relation:

$$p = p_{ext} + \beta(\sqrt{A} - \sqrt{A_0}), \tag{1}$$

where

$$\beta = \frac{2\rho c^2}{\sqrt{A}}$$

with

$$c^2 = \frac{\frac{K}{\rho}}{1 + (\frac{K}{E})(\frac{D}{e})}.$$

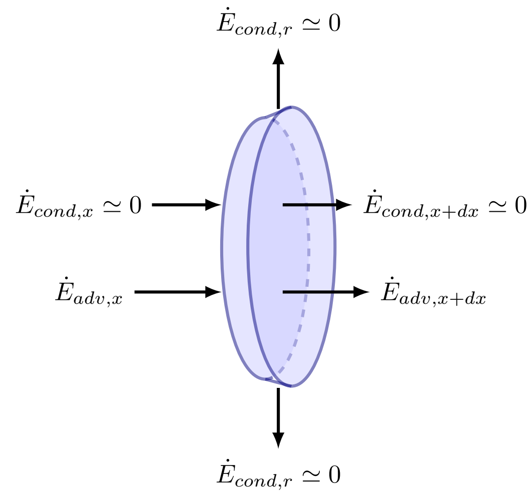

Fig. 1: Control volume for coolant water for an element inside the pipe.

In the above equation, c is the speed of an acoustical wave through the pipe, e is the wall thickness of the pipe, K is the bulk modulus of elasticity of the fluid, and E is the Young's modulus of the elasticity for the wall material. To close the system, two other equations are required, which are provided by the conservation of mass and momentum:

$$\frac{\partial A}{\partial t} + \frac{\partial uA}{\partial x} = 0 \tag{2}$$

$$\frac{\partial u}{\partial t} + \frac{\partial u^2/2}{\partial x} = -\frac{1}{\rho}\frac{\partial p}{\partial x} - \frac{fu^2}{2D} - g\sin\theta \tag{3}$$

In the above equations, f is the friction factor in the pipe and depends on the state of the flow (*i.e.* laminar or turbulent) and the roughness of the pipe wall. The variable θ is the angle between the pipe axis and the horizon.

2) Energy: Following our assumptions, we consider the control volume as shown in Figure 1. The control volume expands to the pipe wall boundary, where energy is exchanged through conduction. Moreover, energy crosses the boundary of the control volume by means of axial conduction and advection. The balance of energy for a generic control volume can be written as:

$$\frac{\partial}{\partial t}\oint_{\mathcal{V}} \rho e dV = \oint_{\mathcal{S}} \dot{E}_{adv} dS + \oint_{\mathcal{S}} \dot{E}_{cond} dS \tag{4}$$

As we mentioned in the previous section, the axial and radial conductions are negligible. Thus: $\oint_{\mathcal{S}} \dot{E}_{cond} dS \simeq 0$.

The axial advection for the control volume shown in Figure 1 is given by:

$$\begin{aligned}\oint_{\mathcal{S}} \dot{E}_{adv} dS &\equiv \dot{E}_{adv,x} - \dot{E}_{adv,x+dx} \\ &= \rho u(e + u^2/2)A_x \\ &\quad - \left\{\rho u(e+u^2/2)A_x + \frac{\partial}{\partial x}\left[\rho u(e+u^2/2)A_x\right]dx\right\} \\ &= -\frac{\partial}{\partial x}\left[\rho u(e+u^2/2)A_x\right]dx\end{aligned} \tag{5}$$

Therefore the energy equation becomes:

$$\rho c_p\left(\frac{\partial \Gamma}{\partial t} + \frac{\partial (u\Gamma)}{\partial x}\right) = 0. \tag{6}$$

where $\Gamma = TA$.

The system of partial differential equations for hydrodynamics and heat transfer can be expressed as:

$$\frac{\partial \mathbf{U}}{\partial t} + \mathbf{H}\frac{\partial \mathbf{U}}{\partial x} = \mathbf{F} \tag{7}$$

where:

$$\mathbf{U} = \begin{pmatrix} A \\ u \\ \Gamma \end{pmatrix}, \tag{8}$$

$$\mathbf{H} = \begin{pmatrix} u & A & 0 \\ \frac{1}{\rho D A} & u & 0 \\ 0 & \Gamma & u \end{pmatrix} \tag{9}$$

and

$$\mathbf{F} = \begin{pmatrix} 0 \\ -\frac{1}{\rho}\frac{\partial p}{\partial x} - \frac{fu^2}{2D} - g\sin\theta \\ 0 \end{pmatrix}, \tag{10}$$

Given that $A > 0$, the matrix $\mathbf{H}$ has three real eigenvalues. Thus the above system can be diagonalized to the following form:

$$\frac{\partial \mathbf{W}}{\partial t} + \mathbf{\Lambda}\frac{\partial \mathbf{W}}{\partial x} = \mathbf{S} \tag{11}$$

where:

$$\mathbf{W} = \begin{pmatrix} W_1 \\ W_2 \\ W_3 \end{pmatrix},$$

with W_1, W_2 and W_3 being the Riemann invariants given by:

$$W_1(\mathbf{H}) = u + 4(c - c_0) = u + 4\sqrt{\frac{\beta}{2\rho}}(A^{1/4} - A_0^{1/4}) \tag{12}$$

$$W_2(\mathbf{H}) = u - 4(c - c_0) = u - 4\sqrt{\frac{\beta}{2\rho}}(A^{1/4} - A_0^{1/4}) \tag{13}$$

$$W_3(\mathbf{H}) = \Gamma/A \tag{14}$$

and $\mathbf{\Lambda}$ is a diagonal matrix whose entries are:

$$\lambda_1(\mathbf{H}) = u + c; \qquad \lambda_2(\mathbf{H}) = u - c; \qquad \lambda_3(\mathbf{H}) = u. \tag{15}$$

In most piping network systems, $c >> u$, and therefore $u+c > 0$ and $u-c < 0$. As a result the characteristic curve that is obtained from $dx/dt = u + c$ is *forward traveling* and the characteristic curve with $dx/dt = u-c$ is *backward traveling*. The characteristic curve obtained by $dx/dt = u$ can be either forward traveling or backward traveling depending on the sign of u.

C. Component Modeling

1) One-to-One Connector: A One-to-One Connector is a component that links two pipes and provides boundary conditions for the end of the connecting pipes. Pumps, valves, bends and heat exchangers are such components. These components are modeled as *zero-dimensional*. The schematic of the component and the connecting pipes is

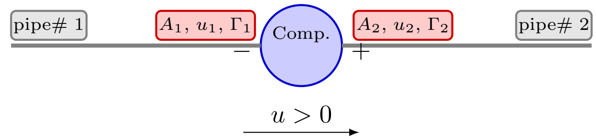

Fig. 2: The schematic of the one-to-one component model.

shown in Figure 2. The six unknowns are shown in red. These variables are A_1, u_1 and Γ_1 from pipe #1, and A_2, u_2 and Γ_2 from pipe #2. The hydrodynamic variables A_1, A_2, u_1, and u_2, are independent of temperature and they can be solved separately. Thus we need four equations to close the system. Forward traveling characteristic waves carry information to the component through pipe # 1, and backward traveling characteristic waves carry information to the component through pipe # 2. These two Riemann invariants provide two independent equations. The conservation of mass provides the third equation. The fourth equation is obtained by incorporating the total pressure change, denoted by ΔP_t, for fluid traveling from pipe #1 to pipe #2. In summary these four equations are:

$$u_1 + 4\sqrt{\frac{\beta}{2\rho}}(A_1^{1/4} - A_0^{1/4}) = W_1 \tag{16}$$

$$u_2 - 4\sqrt{\frac{\beta}{2\rho}}(A_2^{1/4} - A_0^{1/4}) = W_2 \tag{17}$$

$$A_1 u_1 = A_2 u_2 \tag{18}$$

$$(P_2 + \frac{1}{2}u_2^2) - (P_1 + \frac{1}{2}u_1^2) = \Delta P_t \tag{19}$$

The pressure change depends on the component. For instance, for pumps, ΔP_t represents the pressure increase imparted by the pump, and thus $\Delta P_t := P_p(Q)$ where $P_p(Q)$ is the pump characteristic curve as a function of volumetric flow rate $Q = A_1u_1 = A_2u_2$. For valves, bends and heat exchangers, ΔP_t represents the pressure loss as flow travels through these components and thus it is generically expressed as: $\Delta P_t = -\frac{K}{2}\rho u|u|$, where $K \geq 0$ is the loss coefficient.

Note that the pressure is algebraically related to area through the constitutive model given by Equation 1.

To solve for Γ_1 and Γ_2 we use the balance of energy and the characteristic equations. The balance of energy for the component can be written as:

$$\dot{Q}_t = \dot{m}c_p(T_2 - T_1)$$

In this setting, $\dot{Q}_t$ is the amount of total heat transfered to the component. Substituting for $\dot{m} = \rho u_1 A_1 = \rho u_2 A_2$ and the definitions of $\Gamma_1 = T_1 A_1$ and $\Gamma_2 = T_2 A_2$, we arrive at:

$$\dot{Q}_t = \rho c_p(u_2\Gamma_2 - u_1\Gamma_1)$$

To close the system, we use the information that propagates along the characteristic $dx/dt = u$. This follows:

$$\begin{aligned} &\text{if} \quad u \geq 0, \quad T_1 = W_3 \\ &\text{if} \quad u < 0, \quad T_2 = W_3. \end{aligned}$$

We assume that pumps, valves and bends are adiabatic and therefore $\dot{Q}_t = 0$ for these components. For heat exchangers, *i.e.* heat loads and chillers, $\dot{Q}_t$ is either calculated from a reduced order model or it is assumed to be given.

2) One-to-Two Connector: One-to-two connector links three pipes at a *junction*. The modeling of a junction is similar to the one-to-one connector with nine unknowns. The junctions could be of splitting or merging type. For more details on the modeling of the junctions see reference [3].

D. Numerical Method

We use Discontinuous Galerkin (DG) method to discretize the system of partial differential equations given by equation 7. We split each pipe to Ne elements and within each element Legendre polynomials are used as the basis. We use upwinded flux that propagates information between the elemental regions and the bifurcations of the system. The equations for components form a nonlinear system of equations that are solved at every time step using the Newton-Raphson method. An Adams-Bashforth scheme is used for the time integration. A brief outline of the numerical method introduced in [3] is presented here. For more details on the numerical method see [4].

III. Demonstration case

In this section, we use the computational tool to analyze the performance of a cooling pipe network aboard a modern naval ship. In the following we describe the problem inputs and the design parameters and then we discuss the results.

A. Inputs

1) Geometric parameters: The overall length of the ship is $L_S = 167.29(m)$, and the overall beam is $L_B = 20.34(m)$. We place the coordinate system at the center of the ship with the longitudinal coordinate, x, expanding from $-L_S/2$ to $L_S/2$.

2) Heat loads: There are 26 heat loads aboard the ship. We have considered the maximum values that the heat loads can acquire in different modes of operation. For the sake of simplicity, we have divided the ship into six equal longitudinal segments, or zones, and lumped all the loads that lie in each zone into a single load. The value of the lumped load is equal to the summation of all heat loads that lie within that segment, as shown in Table I.

3) Physical parameters: The Young's modulus of the pipe is $E = 1.84 \times 10^{11}(Pa)$, and the ratio of the pipe diameter to its thickness is assumed to be $D/e = 8$ for all pipes. The bulk modulus of elasticity for water is $K = 2.39 \times 10^{11}(Pa)$. The density of water is $\rho = 1028(kg/m^3)$. The flow regime in all pipes is assumed to be turbulent and the friction factor is set to be constant at $f = 0.04$ for all pipes.

TABLE I: Lumped values of heat loads and their locations.

Identifier	$\dot{Q}(kW)$	$x(m)$	$y(m)$	$z(m)$
1	532	-66.67	-0.34	6.76
2	5050	-40.00	0.00	16.57
3	4723	-13.34	-0.08	18.27
4	2611	13.34	0.43	16.95
5	153	40.00	-2.00	5.41
6	378	66.67	2.00	0.01

B. Design variables

1) Thermal zones: Six thermal zones are considered, and two chillers are placed in each zone. The zonal boundaries and chillers are shown in Figure 3.

2) Pipe configuration: A *simple loop* layout is considered for the supply and return header; see [1] for more details and other options. The port and starboard main piping heights are 5.20 (m) and 10.20 (m), respectively. The offset between the supply and return header is 0.50 (m).

The supply and return *branch* piping connect each heat load to the corresponding headers. We model each branch as a two-pipe segment with a single 90-degree bend in the $(y - z)$ plane; all flow in the x direction occurs in the headers.

3) Pipe/pump sizing: The pipe diameter for each branch is proportional to the corresponding heat load, $\dot{Q}$. As an initial estimate, we use the parametric equation introduced in reference [2]:

$$D = (\frac{4K\dot{Q}}{C\pi})^{0.4}. \tag{20}$$

The diameter is then rounded to the closest standard sizing for pipes. The diameter of the main supply/return header is $D_h = 14$ (inches). The supply pumps are located at the exit of each chiller. Therefore we have a total of twelve pumps. The pumps are all identical with the characteristic curve obtained from curve-fitting the empirical data as shown in Figure 4.

C. Results

We assume that the chilled water temperature is always kept constant at $T_{chill} = 279.817K = 44F$. This can be achieved by setting the temperature at chiller outlet at $279.817K$. Since we assume that the pipes are adiabatic, we expect to preserve this temperature in the supply pipes. In this fashion, we can measure the cooling capacity required at each chiller to always maintain the supply chilled water temperature at $T = 279.817K$. We initialize the temperature of all pipes at $t = 0$ to $T = 279.817K$.

In Figure 5, the coolant mass flow rate of three chillers versus time is shown. Chillers $\mathcal{CH}_1$ and $\mathcal{CH}_2$ both belong to the same thermal zone, but due to the asymmetry of the

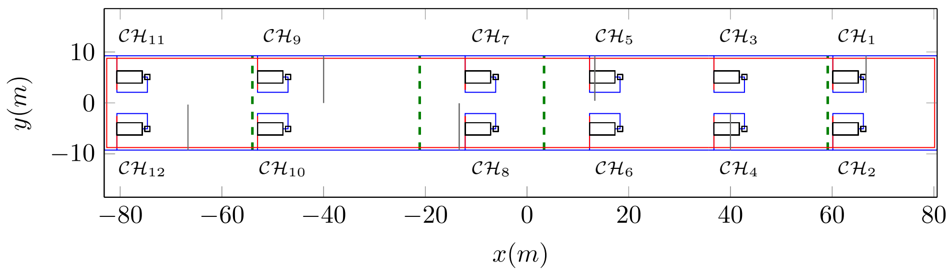

Fig. 3: Double main piping system with branches (plan view). Zonal boundaries are shown with dashed green line. the supply/return to heat loads are shown with gray line.

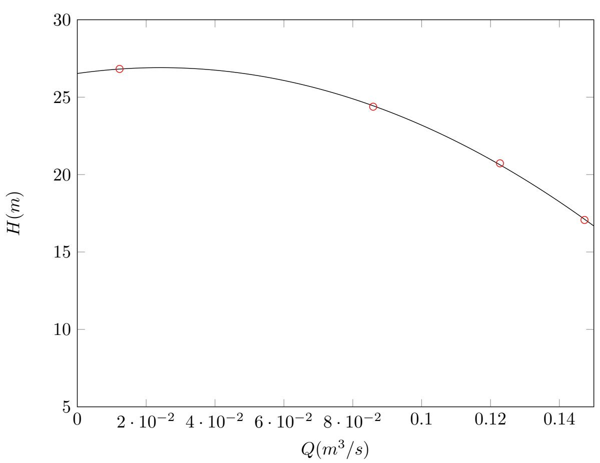

Fig. 4: Pump characteristic curve chosen for the coolant network. The circles show the empirical data provided by the pump manufacturer. The solid line shows a parabolic curve fit to the data points.

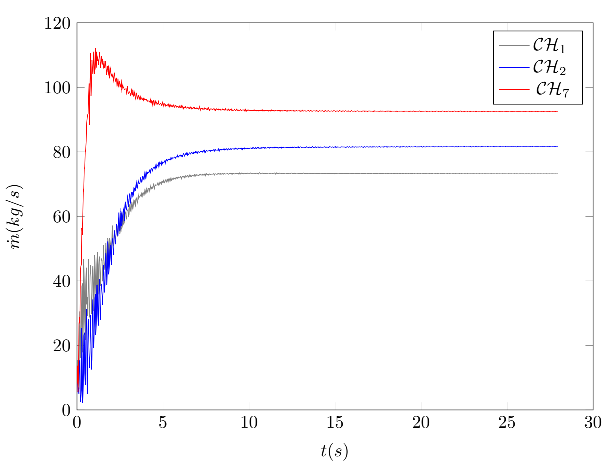

Fig. 5: Chilled water mass flow rate at three different chillers versus time.

pipe network, these two chillers have different mass flow rates. All three chillers show convergence to a steady state after a transient period. The "high-frequency" oscillations observed in the mass flow rate signal, are the result of acoustic wave propagation throughout the pipe network. Since $c >> u$, these oscillations appear on much smaller time scales than the inertial time scale of the flow, *i.e.* D/u.

The primary objective of the current simulation is to compute how much cooling capacity each chiller requires to remove the heat from the loads in the steady operation. In Figure 6 the instantaneous cooling capacity of all twelve chillers are shown. For the sake of clarity, the plot is divided into three plots with four chillers shown in each plot. The cooling capacity shown in Figure 6 represents the amount of heat that must be removed by each chiller to maintain the supply water temperature at T_{chill}. As it is shown in Figure 6, each chiller experiences a sudden rise in $\dot{Q}$, after some initial interval, which is due to the time it takes for the return water to travel from the heat load back to the chillers. However, after the sudden rise, the demand for cooling capacity settles to the steady-state values.

Comparing the the total cooling capacity of all chillers versus the total heat load provides a robust verification check for the numerical computation carried out in this section. In Figure 7, the total cooling capacity of the cooling network is compared with the total heat load. The total heat load is obtained by adding up the heat loads given in table I. This value is $\dot{Q}_{load} = 13.35(MW)$. It is clear that the total cooling capacity converges to this value.

D. Analysis

The highest capacity is $\dot{Q} = 1.66(MW)$ and it belongs to the third chiller. It is often preferred to choose identical chillers for all thermal zones due to lower installation and maintenance costs. Thus for the current ship we would need twelve chillers with the cooling capacity close to $1.66(MW)$, which is an order of magnitude increase compared to conventional ships. A state-of-the-art chiller with the cooling capacity of $1.5(MW)$, has a volume of $5.00(m) \times 2.40(m) \times 2.30(m)$ and it weighs 20000 kg. (See for instance York, Sea Water Cooled Centrifugal AC). Therefore the total volume and weight of the chillers roughly become 331 m^3 and 24 tons. Moreover, a ship with

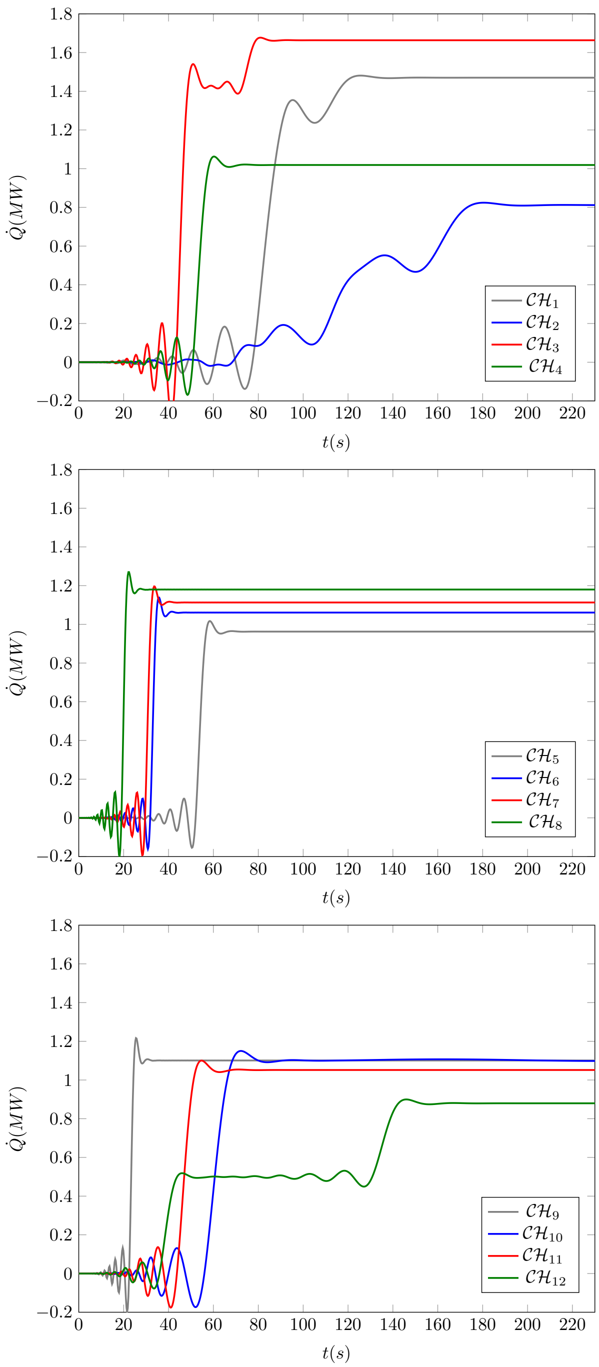

Fig. 6: Cooling capacity for all twelve chillers versus time. For clarity, only four chillers are shown in each plot. The coolant capacity is required to maintain the chilled water at $T = T_{chill}$. The cooling capacity eventually reaches steady-state values. The steady-state capacities are different for different chillers, and it varies from 0.88 MW at $\mathcal{CH}_{12}$ to 1.66 MW at $\mathcal{CH}_3$.

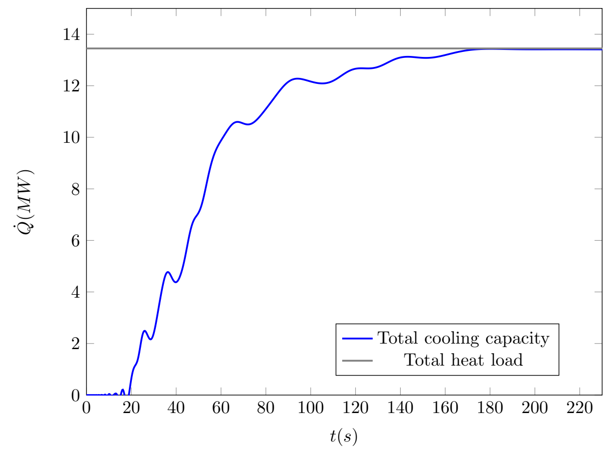

Fig. 7: The total cooling capacity of all twelve chillers compared with the total heat load of $\dot{Q} = 13.45(MW)$.

the current design would suffer from high vulnerability as $\mathcal{CH}_7$ and $\mathcal{CH}_8$, and $\mathcal{CH}_9$ and $\mathcal{CH}_{10}$ are unable to sustain the heat generated within the thermal zones they are located in. The current design can only handle all the heat loads with all chillers operating concurrently.

IV. Conclusion

We developed a computational tool that is suitable for the early stages of design. Applying our computational tool to evaluate the performance of a proposed cooling network, we highlighted some of the challenges in using the state-of-the-art technology for cooling modern naval ships with high heat loads.

References

[1] A. B. Sanfiorenzo, "Cooling system design tool for rapid development and analysis of chilled water systems aboard U.S. Navy surface ships," Engineer's thesis, Massachusetts Institute of Technology, 2013.

[2] E. R. Fiedel, J. S. Chalfant, and C. Chryssostomidis, "Cooling system early-stage design tool for naval applications," in *Proceedings of the 2011 Grand Challenges in Modeling and Simulation, GCMS '11*, The Hague, Netherlands, June 27-29, 2011.

[3] S. Sherwin, V. Franke, J. Peiro, and K. Parker, "One-dimensional modelling of a vascular network in space-time variables," *Journal of Engineering Mathematics*, vol. 47, no. 3-4, pp. 217–250, 2003.

[4] B. Cockburn and C.-W. Shu, "The Runge–Kutta discontinuous Galerkin method for conservation laws V: Multidimensional systems," *Journal of Computational Physics*, vol. 141, no. 2, pp. 199–224, 4 1998.